*J Mater Sci: Mater Electron* (2026) 37:2068

# Hydrothermally engineered $CoMoO_4/NiMoO_4$ electrode material for next-generation supercapacitors

S. Sakthivel[1,2,*], B. Kabilan[1,2], Manikandan Ayyar[1,2,*], S. Ananya[1,2], Balaji Krishnasamy[3], D. Shanmugapriya[4], and Lalitha Gnanasekaran[5]

[1] *Department of Chemistry, Karpagam Academy of Higher Education, Coimbatore, Tamil Nadu 641021, India*
[2] *Centre for Material Chemistry, Karpagam Academy of Higher Education, Coimbatore, Tamil Nadu 641021, India*
[3] *Sustainable Materials Research Lab, Department of Chemistry, PSG Institute of Technology and Applied Research, Neelambur, Coimbatore 641062, India*
[4] *Vicerrectoría de Investigación y Postgrado, Universidad de La Serena, Código postal: 1700000 La Serena, Chile*
[5] *International Center of Nanotechnology and Functional Materials, Instituto de Alta Investigación, Universidad de Tarapacá, 1000000 Arica, Chile*

**Received:** 16 April 2026
**Accepted:** 4 September 2026
**Published online:** 20 September 2026

© The Author(s), under exclusive licence to Springer Science+Business Media, LLC, part of Springer Nature, 2026

## ABSTRACT

The development of advanced electrode materials with high capacitance and long-term cycling durability is critical for next-generation supercapacitor applications. Despite the promising properties of individual $CoMoO_4$ and $NiMoO_4$ phases, standalone electrodes suffer from limited rate performance and insufficient cycling stability. To address these limitations, the present work reports the hydrothermal synthesis of $CoMoO_4/NiMoO_4$ composite (CNMO). Structural characterization by X-ray diffraction (XRD) confirmed the formation of a highly crystalline monoclinic phase without detectable impurities. Scanning electron microscopy (SEM) analyses revealed the formation of interconnected nanorods, providing a large electrochemically active surface area and efficient ion diffusion pathways. X-ray photoelectron spectroscopy (XPS) further confirmed the coexistence of mixed-valence Co, Ni, and Mo species, which contribute to enhanced faradaic redox activity and improved charge transfer kinetics. Owing to the synergistic interaction between $CoMoO_4$ and $NiMoO_4$, the CNMO electrode delivered a high specific capacitance (Sc) of 2948 F $g^{-1}$ at 2 A $g^{-1}$ and retained 86% of its initial capacitance after 5000 charge–discharge cycles. Furthermore, an asymmetric supercapacitor device (CNMO//AC) exhibited a specific capacitance of 143 F $g^{-1}$, an energy density of 38.9 Wh $kg^{-1}$ at a power density of 2090 W $kg^{-1}$, and excellent cycling stability with 82% capacitance retention after 5000 cycles. The enhanced electrochemical performance can be attributed to the synergistic

Address correspondence to E-mail: sakthivelsns33001@gmail.com; manikandan.frsc@gmail.com

E-mail Addresses: kabilanvj123@gmail.com; ananyasasikumar602@gmail.com; balaji.psgtech@yahoo.co.in; sdpriyalaserena@gmail.com; lalitha1887@gmail.com

https://doi.org/10.1007/s10854-026-18434-y

redox contribution of the bimetallic molybdate framework and the favorable nanorod architecture. These findings demonstrate that the CNMO composite is a promising electrode material for high-performance energy storage applications.

## 1 Introduction

Energy storage systems that are more dependable and efficient are necessary in the contemporary environment due to the steady introduction of devices with smart technologies and features. Because of its high-power density, long cycle life, and ability to charge and discharge quickly, the supercapacitor is a type of energy storage device that has garnered the most attention [1]. Among portable electronic applications, supercapacitors (SCs), especially, have received a great deal of interest because of their unparalleled high-power density, impressive lifetime, rapid charging and discharging capabilities and reliability [2]. Their special electrochemical performance make them critical for a wide range of wearable electronics, including smartwatches and flexible displays, mobile communication devices, like smartphones and tablets, electric vehicles (EVs) and hybrid electric vehicles (HEVs), portable medical tools, such as implantable drug delivery systems and defibrillators, where regenerative braking and high-speed energy delivery are essential functions [3]. Additionally, the development of the Internet of Things (IoT) has accelerated the application of SCs in energy harvesting systems, wireless sensor networks and smart automation devices, where they are capable of harvesting energy from the environment, like solar cells, piezoelectric generators, and thermoelectric generators, and storing it effectively [4]. Besides, their high-power density and excellent performance in harsh environments are well-suited for advanced military communication systems, unmanned aerial vehicles (UAVs) and satellite power management applications [5]. As a result, researchers have been focusing on the development of new supercapacitor electrode materials that exhibit high electrochemical properties and do not require expensive electrolyte, which has led to the development of a new class of materials that possess high capacitance and can be used in supercapacitors [6].

Among the available energy storage devices, supercapacitors occupy a unique position between conventional dielectric capacitors and batteries. Conventional capacitors can deliver very high-power density and almost unlimited cycle life, but their energy density is too low for most practical energy storage needs. Batteries, on the other hand, offer high energy density but suffer from slow charge–discharge kinetics, limited cycle life caused by irreversible redox/phase-change reactions, and safety concerns such as flammability and thermal runaway [7]. Supercapacitors bridge this gap: they store charge through highly reversible surface or near-surface electrochemical processes rather than bulk redox phase transformations, which allows them to deliver power densities approaching those of conventional capacitors while achieving energy densities far higher than dielectric capacitors, along with markedly faster charge–discharge rates, longer cycle life (often exceeding tens of thousands of cycles), and safer, more stable operation than most battery chemistries [8].

Based on their charge-storage mechanism, supercapacitors can be broadly classified into three types: electrical double-layer capacitors (EDLCs), pseudocapacitors, and hybrid supercapacitors. EDLCs are generally based on carbon materials including activated carbon, carbon nanotubes, and graphene, store charge electrostatically through the accumulation of ions at the electrode–electrolyte interface, without any charge transfer between the electrode and the electrolyte. This non-faradaic mechanism gives EDLCs excellent cycling stability and high-power density, but their specific capacitance and energy density remain comparatively low [9]. Pseudocapacitors, utilize redox-active materials such as transition metal oxides, hydroxides, and conducting polymers, which store charge through rapid and reversible faradaic reactions, including surface redox process and ion intercalation. This faradaic mechanism allows pseudocapacitors to achieve specific capacitance values typically one to two orders of magnitude higher than EDLCs, although they can suffer from comparatively lower electrical conductivity and cycling stability. Hybrid supercapacitors combine an EDLC-type electrode with a pseudocapacitive or battery-type electrode in a single device, harnessing the high-power density of the former and the high energy density of the latter to achieve a favorable overall balance of performance. The composite developed

in the present work falls within the pseudocapacitor category, exploiting the reversible redox activity of transition metal molybdates [10].

Transition metal oxides are among the many electrode materials with high specific capacitance that have garnered a lot of interest and environmental friendliness. Transition metal oxides effectively store energy utilizing highly reversible redox reactions because of the existence of changing valence metal species [11]. Metal molybdates, a novel class of metal oxides, are known for their excellent electrical conductivity, diverse valence states, and stable crystal structure, including $CoMoO_4$, $NiMoO_4$, $ZnMoO_4$, $MnMoO_4$, and $CuMoO_4$, which have led to their exploration as electrode materials in recent years [12].

Among them, $NiMoO_4$ in particular has garnered a lot of interest because of its high redox activity (particularly for the Ni element), chemical stability, low cost, and abundance in nature [13]. Because of its high Ni element activity, $NiMoO_4$ exhibits highest specific capacitance; however, it has low-rate performance and poor cycling stability [14]. $NiMoO_4$ semiconductors are known to be promising materials for electrodes in pseudocapacitors. Their exceptional electrical and thermal conductivity, chemical stability, abundance, and affordability are the reasons for this [15]. For high-performance supercapacitors, morphological optimization, and the development of core–shell heterostructures have been utilized to overcome these problems [16]. Due to its potential uses in fields including photochemistry, ion exchange, intercalation, proton conductivity, and chemistry, the cobalt molybdate ($CoMoO_4$) nanocatalyst has lately attracted interest. Furthermore, at the nanoscale level, studies have been performed to cultivate particles with distinct forms, including nanoneedles, nanowires, and nanotubes. The rationale for combining $CoMoO_4$ and $NiMoO_4$ is now clearly presented as synergistic composite design: $CoMoO_4$ provides structural stability and enhanced conductivity via $Co^{2+}/Co^{3+}$ redox transitions, while $NiMoO_4$ contributes high specific capacitance through $Ni^{2+}/Ni^{3+}$ redox activity. Together, the composite offers superior performance compared to either individual component. The composite of molybdates during development will provide the redox reactions, leading to increased electrochemical performance and enhanced electrical conductivity [17].

Besides transition metal molybdates, rare-earth-based materials, such as cerium oxide ($CeO_2$), lanthanum oxide ($La_2O_3$), and gadolinium oxide ($Gd_2O_3$), have also been explored for supercapacitor electrodes owing to their high redox activity, ion exchange capacity, and good chemical stability, which can enhance the electrochemical performance of host materials when used as dopants in metal oxides or conducting polymers. However, rare-earth elements are not selected as the primary electrode material in the present study for several practical reasons: they are comparatively scarce and geographically concentrated in supply, their extraction and purification require complex, energy-intensive, and environmentally taxing processing, and the resulting materials are typically expensive, which limits their scalability for large-volume electrode fabrication. Moreover, rare-earth compounds are most often employed as minor dopants to enhance the conductivity of an existing host material rather than as standalone high capacitance electrode hosts in their own right [18]. In contrast, the transition metal molybdates used in this study ($NiMoO_4$ and $CoMoO_4$) are naturally abundant, inexpensive, and intrinsically redox-active, making them more suitable for the development of a scalable, low-cost, high-performance composite electrode.

Various chemical synthetic methods can be employed to synthesize molybdate compounds, including sonochemical, hydrothermal methods, and micro-emulsion [19–21]. The synthesis method's physical and chemical characteristics can significantly affect the final nanoparticles' capacitive behavior, surface area, and overall stability; hence, this aspect is crucial [22]. Among these methods, the hydrothermal route was selected for the synthesis of the CNMO in the present work because of its distinct advantages: it is a simple, low-cost, single-step, and environmentally friendly process that does not require sophisticated equipment or hazardous reagents, while still offering precise control over reaction parameters such as temperature, precursor concentration, and reaction time. This level of control allows the morphology, particle size, crystallinity, and porosity of the resulting nanostructures to be finely tuned, which directly governs the electrochemical performance of the final electrode material. The hydrothermal method is also readily scalable, making it well-suited for the reproducible, large-scale synthesis of composite metal molybdate nanostructures such as the CNMO developed here [23]**.** The hydrothermal method was used by Cai et al. to prepare $NiMoO_4$ NRs, which had a capacitance of 974.4 F $g^{-1}$ at 1 current density [24]. Lin et al. prepared $NiMoO_4$ hollow nanorods utilizing a

hydrothermal process to serve as the supercapacitor's positive electrode. The $NiMoO_4$ provided the highest specific capacitance value of 1102.2 F $g^{-1}$ at 1 A/g [25]. Recently, Raj et al. produced $NiMoO_4$ nanoflowers using a co-precipitation method, and achieved 554 C $g^{-1}$ at 1 A $g^{-1}$ [26]. Zhanwei Xu et al. reported that a cobalt molybdate exhibited a Sc value of 171.1 mA h $g^{-1}$ [27]. John Candler et al. reported driven morphology-reliant $CoMoO_4$ and achieved the Sc value of 170 F $g^{-1}$ [28].

Despite these advances, most prior reports on $CoMoO_4$/$NiMoO_4$ systems rely on multi-step, template-assisted, or core–shell fabrication routes, which add synthetic complexity and cost. The key novelty of the present study lies in the development of a facile, one-pot hydrothermal synthesis of $CoMoO_4$/$NiMoO_4$ (CNMO) in a single reaction vessel, followed by a single thermal treatment step to enhance crystallinity, eliminating the need for multi-step or template-assisted procedures reported elsewhere. This simplified strategy directly combines the structural stability and conductivity benefits of $CoMoO_4$ with the high specific capacitance of $NiMoO_4$ within a single nanorod architecture, offering a scalable and cost-effective pathway toward high-performance pseudocapacitive electrodes.

In this work, the synthesis of CNMO and its electrochemical performance were evaluated. The conductive properties and synergistic effect materials of $CoMoO_4$ and $NiMoO_4$. The facile preparation method consisted of producing the required substance in a single reaction vessel and then applying heat to improve its crystallinity. The synthesized samples were analyzed using FT-IR, TEM, XRD, and XPS methods, which confirmed the successful formation of the CNMO with the expected nanorod morphology and crystal structure. Their electrochemical properties were analyzed through Electrochemical impedance spectroscopy (EIS), cyclic voltammetry (CV), and galvanostatic charge and discharge (GCD). In a three-electrode supercapacitor system, electrochemical characterisations were performed using a 6 M potassium hydroxide aqueous solution, and the CNMO electrode delivered a high specific capacitance of 2948 F $g^{-1}$ at 2 A $g^{-1}$, along with 86% capacitance retention after 5,000 cycles, confirming its excellent rate capability and cycling stability. To further evaluate its practical applicability, a two-electrode asymmetric supercapacitor device was assembled using the CNMO electrode, which achieved an energy density of 38.9 Wh $kg^{-1}$ at a power density of 2090 W $kg^{-1}$, demonstrating the material's potential for real-world energy storage applications. Given this combination of high capacitance, good cycling stability, and favorable energy/power characteristics, the developed CNMO holds strong promise for use in portable and wearable electronics, electric and hybrid electric vehicles, and other next-generation energy storage applications requiring fast charge–discharge capability and long operational life.

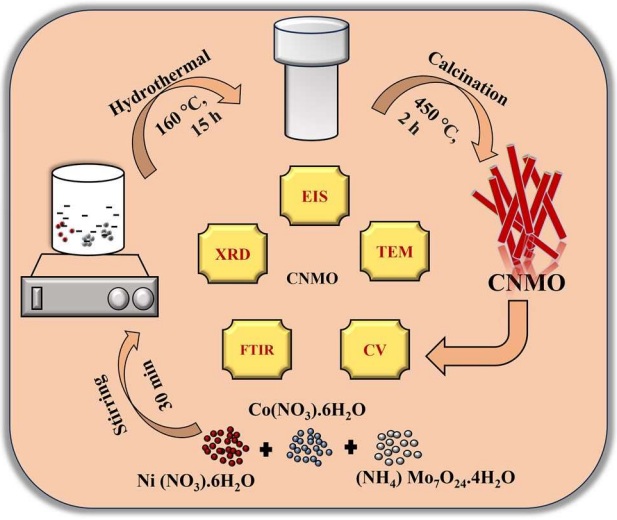



**Fig. 1** Schematic diagram of the CNMO

## 2 Experimental section

### 2.1 Materials

Ammonium molybdate tetrahydrate, potassium hydroxide, HCl, and cobalt nitrate hexahydrate and nickel nitrate hexahydrate, were purchased from Sigma–Aldrich. Vritra Technologies was the source of the nickel foam. The purchased chemicals were used without any further purification.

### 2.2 Hydrothermal synthesis of CNMO

$CoMoO_4$/$NiMoO_4$ (CNMO) nanorod electrode material was fabricated directly onto the cleaned nickel foam by a facile one-step hydrothermal reaction in an autoclave, which is schematically illustrated in Fig. 1. Initially, the nickel foam (2 × 2 $cm^2$, 1.6 mm thick, 95% porosity) was sequentially ultrasonicated in 3 M

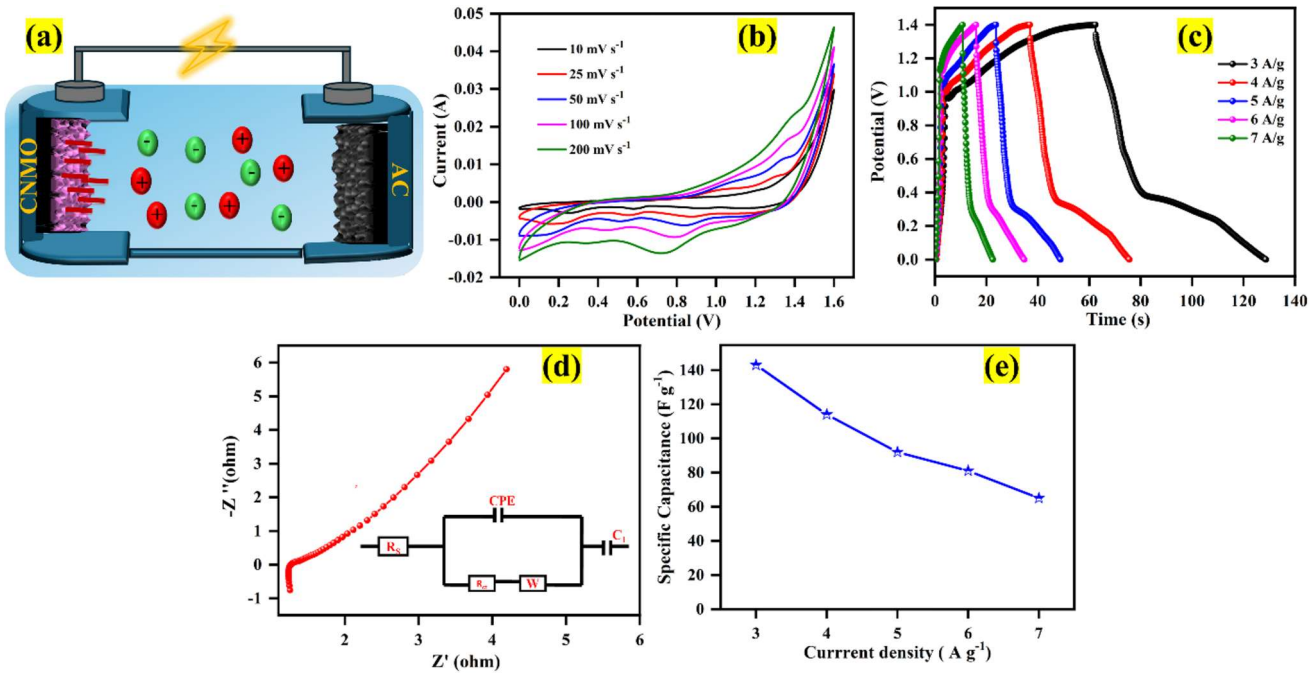



**Fig. 9** **a** Schematic diagram of CNMO//AC device, **b** CNMO//AC CV analysis, **c** CNMO//AC GCD analysis, **d** CNMO//AC EIS spectra, and **e** Current density vs Specific capacitance plot

between 3 and 7 A $g^{-1}$ within an active potential range of 0 to 1.4 V. Typical non-linear charge–discharge curves in Fig. 9(c) display the charge stored by the slow faradaic redox process [52]. GCD at various current densities showed that the maximum capacitance of the CNMO//AC hybrid device is 143, 114, 92, 81, and 65 F $g^{-1}$ at 3, 4, 5, 6, and 7 A $g^{-1}$, respectively, as shown in Fig. 9(e).

The developed device's cycling of stability is displayed in Fig. 10(a). The device shows extraordinary cyclic stability even after 5000 cycles, maintaining 82% of its capacitance and 93% of the coulombic efficiency. The electrochemical analysis to demonstrate capacitive behavior, energy, and power densities is required. The Ragone plot of the CNMO//AC hybrid device, is presented in Fig. 10(b). Ragone plots were calculated based on the total active mass of both positive (CNMO) and negative (activated carbon) electrodes, the CNMO//AC hybrid device delivered a maximum energy density of 38.9 Wh $kg^{-1}$ and power density of 2090 W $kg^{-1}$ at 3 A $g^{-1}$ respectively, as shown in Fig. S3. The higher energy density values (31, 25.4, 22.5, and 17 Wh $kg^{-1}$) and higher power density values (2936, 3600, 4400, and 5100 W $kg^{-1}$) were demonstrated by the hybrid gadgets at current densities between 4 and 7 A $g^{-1}$ [53].

## 4 Conclusions

In this study, CNMO was synthesized via a facile one-pot hydrothermal route, and evaluated as a supercapacitor electrode material. XRD analysis were confirmed the crystalline, monoclinic phase, while electron microscopy revealed an interconnected nanorod morphology. XPS verified the coexistence of mixed-valence Co, Ni, and Mo species, confirming successful integration of both molybdate phases. This structure directly underpins the observed performance. The interconnected nanorods provide a high electrochemically active surface area and short ion-diffusion pathways, facilitating rapid electrolyte access and faradaic charge transfer, while their continuous network ensures efficient electron transport to the nickel foam current collector. Simultaneously, the mixed-valence $Co^{2+}/Co^{3+}$ and $Ni^{2+}/Ni^{3+}$ redox couples provide multiple, closely coupled faradaic pathways, allowing the high capacitance of $NiMoO_4$ and the conductive, structurally stable framework of $CoMoO_4$ to act synergistically rather than additively. This structure–property synergy is reflected in the CNMO electrode specific capacitance of 2948 F $g^{-1}$ at 2 A $g^{-1}$ and 86% capacitance retention after 5000 charge-discharge cycles. The assembled CNMO//AC hybrid

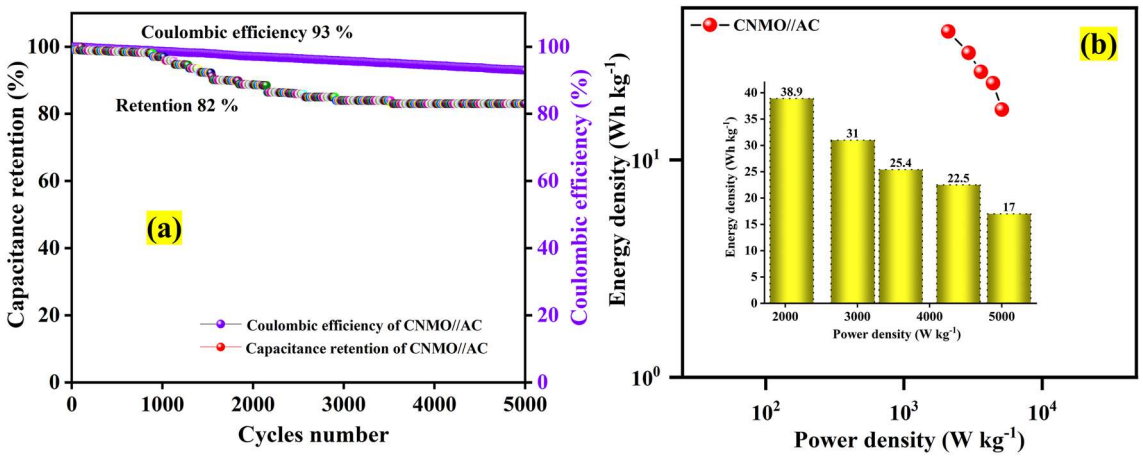



**Fig. 10** **a** Capacitance retention and coulombic efficiency plot, **b** Ragone plot of CNMO//AC hybrid device (inset: bar chart of energy density values at different power densities)

device achieved 143 F $g^{-1}$, an energy density of 38.9 Wh $kg^{-1}$ at 2090 W $kg^{-1}$, and 82% retention after 5000 cycles, confirming that the nanorod architecture and bimetallic redox activity. These results demonstrate that the enhanced electrochemical response of CNMO originates from the coupling of its crystalline, high-surface-area nanorod morphology with synergistic multi-valence redox chemistry, supporting bimetallic molybdate composite design as an effective strategy for low-cost, high capacitance, durable electrode materials for next-generation energy storage applications.

## Author contributions

S. Sakthivel, B. Kabilan, Manikandan Ayyar: Conceptualization, Data curation, Formal Analysis, Funding acquisition, Investigation, Methodology, Project administration, Resources, Software, Supervision, Validation, Visualization, Writing—original draft, and Writing—review & editing; S. Ananya, Balaji Krishnasamy: Data curation, Formal Analysis, Investigation, Methodology, Validation, Visualization, Writing—original draft, and Writing—review & editing; Manikandan Ayyar, D. Shanmugapriya, Lalitha Gnanasekaran: Validation, Visualization, and Writing—review & editing; All authors have read and agreed to the published version of the manuscript.

## Funding

No funding was received from any source.

## Data availability

No datasets were generated or analysed during the current study.

## Declarations

**Competing interests** The authors declare that they have no known competing financial interests or personal relationships that could have appeared to influence the work reported in this paper.

**Ethical approval** Not applicable.

**AI statement** There is no AI tool used in the manuscript.

**Supplementary Information** The online version contains supplementary material available at https://doi.org/10.1007/s10854-026-18434-y.

## References

1. J. Libich, J. Máca, J. Vondrák, O. Čech, M. Sedlaříková, J. Energy Storage **17**, 224 (2018)
2. N.I. Jalal, R.I. Ibrahim, M.K. Oudah, J. Phys. Conf. Ser. **1973**, 012015 (2021)
3. P. Simon, Y. Gogotsi, Nat. Mater. **19**, 1151 (2020)

4. Z. Bi, Q. Kong, Y. Cao, G. Sun, F. Su, X. Wei, X. Li, A. Ahmad, L. Xie, C.-M. Chen, J. Mater. Chem. A **7**, 16028 (2019)
5. P. Liu, W. Liu, Y. Huang, P. Li, J. Yan, K. Liu, Energy Storage Mater. **25**, 858 (2020)
6. B. Sun, S. Wang, M. Zhang, Polymers **15**, 4538 (2023)
7. C.V.V.M. Gopi, S. Alzahmi, M.Y. Al-Haik, Y.A. Kumar, F. Hamed, Y. Haik, I.M. Obaidat, Mater. Today Sustain. **28**, 100981 (2024)
8. X. Liu, F. Xu, Z. Li, Z. Liu, W. Yang, Y. Zhang, H. Fan, H.Y. Yang, Coord. Chem. Rev. **464**, 214544 (2022)
9. S.N. Ansari, M. Saraf, Z. Abbas, S.M. Mobin, Nanoscale **15**, 13546 (2023)
10. G. Zan, S. Li, P. Chen, K. Dong, Q. Wu, T. Wu, ACS Cent. Sci. **10**, 1283 (2024)
11. M. Popovych, I.M. Budzulyak, V.O. Kotsyubynsky, O.V. Popovych, B.I. Rachiy, R.V. Ilnytskyi, L.S. Yablon, Phys. Chem. Solid St. **21**, 650 (2020)
12. F. Wu, Q. Liao, F. Cao, L. Li, Y. Zhang, Nano Energy **34**, 8 (2017)
13. Z. Yin, Y. Chen, Y. Zhao, C. Li, C. Zhu, X. Zhang, J. Mater. Chem. A **3**, 22750 (2015)
14. H. Chen, S. Chen, Y. Zhu, C. Li, M. Fan, D. Chen, G. Tian, K. Shu, Electrochim. Acta **190**, 57 (2016)
15. S. Arshadi Rastabi, R. Sarraf Mamoory, N. Blomquist, M. Phadatare, H. Olin, Batteries **6**, 5 (2020)
16. X. Zhang, L. Wei, X. Guo, Chem. Eng. J. **353**, 615 (2018)
17. Y. Li, S. Zhang, M. Ma, X. Mu, Y. Zhang, J. Du, Q. Hu, B. Huang, X. Hua, G. Liu, E. Xie, Z. Zhang, Chem. Eng. J. **372**, 452 (2019)
18. S. Liang, H. Wang, Y. Li, H. Qin, Z. Luo, B. Huang, X. Zhao, C. Zhao, L. Chen, Sustain. Energy Fuels **4**, 3825 (2020)
19. K. Seevakan, A. Manikandan, P. Devendran, Y. Slimani, A. Baykal, T. Alagesan, Ceram. Int. **44**, 20075 (2018)
20. S. Sahoo, K. Krishnamoorthy, P. Pazhamalai, V.K. Mariappan, S.-J. Kim, Int. J. Hydrogen Energy **43**, 12222 (2018)
21. H.-J. Kim, D.-J. Kim, T. Anitha, A.K. Yedluri, J.-S. Bak, I. Cho, M. Jagadeesh, A.E. Reddy, New J. Chem. **43**, 15605 (2019)
22. S. Sakthivel, S. Shobika, A. Dinesh, K. Yogalakshmi, R. Suriyaprakash, B. Kabilan, P. Sathyajith, S. Elumalai, L. Gnanasekaran, M. Ayyar, M. Santhamoorthy, Result. Chem. **13**, 101956 (2025)
23. M. AB. Turkia and T. A. Salman, J. Chem. Rev. (2024).
24. D. Cai, D. Wang, B. Liu, Y. Wang, Y. Liu, L. Wang, H. Li, H. Huang, Q. Li, T. Wang, A.C.S. Appl, Mater. Interfaces **5**, 12905 (2013)
25. L. Lin, T. Liu, J. Liu, R. Sun, J. Hao, K. Ji, Z. Wang, Appl. Surf. Sci. **360**, 234 (2016)
26. C.J. Raj, R. Manikandan, K.H. Yu, G. Nagaraju, M.-S. Park, D.-W. Kim, S.Y. Park, B.C. Kim, Inorg. Chem. Front. **7**, 369 (2020)
27. Y. Zhao, Z. Xu, H. Fu, R. Xiao, M. Fu, H. Yue, J. Huang, J. Electrochem. Soc. **167**, 080528 (2020)
28. J. Candler, T. Elmore, B.K. Gupta, L. Dong, S. Palchoudhury, R.K. Gupta, New J. Chem. **39**, 6108 (2015)
29. L.-Q. Mai, F. Yang, Y.-L. Zhao, X. Xu, L. Xu, Y.-Z. Luo, Nat. Commun. **2**, 381 (2011)
30. H. Oudghiri-Hassani, F. Al Wadaani, Molecules **23**, 273 (2018)
31. A.G. Al Lafi, J. Al Abdullah, J. Mol. Struct. **1093**, 13 (2015)
32. Z.K. Heiba, M. Abdellatief, M.B. Mohamed, A. Badawi, J. Mater. Sci. Mater. Electron. **36**, 330 (2025)
33. Z.K. Heiba, N.M. Farag, A. Badawi, M.B. Mohamed, J. Mater. Sci. Mater. Electron. **36**, 510 (2025)
34. P. Dhandapani, P.K. Nayak, A. Maruthapillai, Mater. Chem. Phys. **297**, 127287 (2023)
35. W. Zhou, J. Wu, C. Ouyang, Y. Gao, X. Xu, Z. Huang, J. Appl. Phys. **115**, 093512 (2014)
36. M. Cheng, H. Fan, Y. Song, Y. Cui, R. Wang, Dalton Trans. **46**, 9201 (2017)
37. H. Zhang, Y. Lu, C.-D. Gu, X.-L. Wang, J.-P. Tu, CrystEngComm **14**, 7942 (2012)
38. G. Tai, T. Zeng, J. Yu, J. Zhou, Y. You, X. Wang, H. Wu, X. Sun, T. Hu, W. Guo, Nanoscale **8**, 2234 (2016)
39. M. Mieszkowska, M. Grdeń, J. Solid State Electrochem. **25**, 1699 (2021)
40. J. Cao, L. Li, Y. Xi, J. Li, X. Pan, D. Chen, W. Han, Sustain. Energy Fuels **2**, 1350 (2018)
41. A.K. Mohammed, J.N. Hausmann, S. Gaber, P.P. Sánchez, F. Gándara, K. Laun, I. Zebger, P.W. Menezes, D. Shetty, J. Colloid Interface Sci. **694**, 137630 (2025)
42. J.L. White, F.S. Gittleson, M. Homer, F. El Gabaly, J. Phys. Chem. C **124**, 16508 (2020)
43. M. Görlin, J. Ferreira De Araújo, H. Schmies, D. Bernsmeier, S. Dresp, M. Gliech, Z. Jusys, P. Chernev, R. Kraehnert, H. Dau, P. Strasser, J. Am. Chem. Soc. **139**, 2070 (2017)
44. T. Deng, W. Zhang, O. Arcelus, J.-G. Kim, J. Carrasco, S.J. Yoo, W. Zheng, J. Wang, H. Tian, H. Zhang, X. Cui, T. Rojo, Nat. Commun. **8**, 15194 (2017)
45. M. Fahim, A.U.H.A. Shah, S. Bilal, Materials **12**, 1626 (2019)
46. A.S. Kiran, E.G. Shankar, M. Nagaraju, JSu. Yu, ChemSusChem **18**(15), e202500588 (2025)
47. G. Zhao, M. Sedki, S. Ma, C. Villarreal, A. Mulchandani, D. Jassby, Sensors **20**, 6085 (2020)

48. A. Surya Kiran, B. Ramulu, S. Junied Arbaz, E. Girija Shankar, M. Nagaraju, J.S. Yu, Inorg. Chem. Front. **10**, 2075 (2023)
49. H. Watanabe, S. Omoto, Y. Hoshi, I. Shitanda, M. Itagaki, J. Power. Sources **507**, 230258 (2021)
50. H. Chevulamaddi, V.R. Kalagadda, Mater. Today Sustain. **29**, 101054 (2025)
51. D. Chu, X. Zhao, B. Xiao, A. Libanori, Y. Zhou, L. Tan, H. Ma, H. Pang, X. Wang, Y. Jiang, J. Chen, Chem. A Eur. J. **27**, 8337 (2021)
52. A.R. Mule, B. Ramulu, S.J. Arbaz, A. Kurakula, J.S. Yu, J. Energy Chem. **88**, 579 (2024)
53. M. Kuku, S. Althahban, M. Arishi, Inorg. Chem. Front. **11**, 8258 (2024)

**Publisher's Note** Springer Nature remains neutral with regard to jurisdictional claims in published maps and institutional affiliations.

Springer Nature or its licensor (e.g. a society or other partner) holds exclusive rights to this article under a publishing agreement with the author(s) or other rightsholder(s); author self-archiving of the accepted manuscript version of this article is solely governed by the terms of such publishing agreement and applicable law.